

Enhanced ethanol oxidation on PbO_x -containing electrode materials for fuel cell applications

Hugo B. Suffredini^{b,*}, Giancarlo R. Salazar-Banda^a, Luis A. Avaca^a

^a Instituto de Química de São Carlos, Universidade de São Paulo, C.P. 780, 13560-970 São Carlos, SP, Brazil

^b Universidade Federal do ABC, Centro de Ciências Naturais e Humanas, Rua Santa Adélia 166, Bairro Bangu, Santo André, SP, Brazil

Received 13 April 2007; received in revised form 24 May 2007; accepted 4 June 2007

Available online 23 June 2007

Abstract

The synthesis, characterization and utilization of lead oxide-based catalysts, deposited by the sol–gel method on carbon powder to be used as anode in direct ethanol fuel cells (DEFC) is described. For comparison, other materials, based on Ru and Ir (and mixtures of Ru, Ir or Pb) were tested in the same experimental conditions. X-ray diffraction analysis showed that the Pb was deposited on carbon powder as a mixture of PbO and PbO_2 molecular structures. The catalysts $\text{Pt}(\text{RuO}_2\text{-PbO}_x)$ and $\text{Pt}(\text{RuO}_2\text{-IrO}_2)$ exhibited significantly enhanced catalytic activity for the ethanol oxidation as compared to Pt/C commercial powder. Quasi-steady-state polarization curves showed that the composites $\text{Pt}(\text{RuO}_2\text{-PbO}_x)/\text{C}$ and $\text{Pt}(\text{RuO}_2\text{-IrO}_2)/\text{C}$ started the oxidation process in very low potentials (155 and 178 mV, respectively). So, the addition of metallic oxides by the sol–gel route to Pt is presented as a very interesting way to prepare materials with high catalytic activity for direct ethanol fuel cell systems. Current–time studies also showed the good performance of the $\text{Pt}(\text{RuO}_2\text{-PbO}_x)$ catalyst due to smaller poisoning of the material as the process advances.

© 2007 Elsevier B.V. All rights reserved.

Keywords: Lead oxide-based catalysts; Pb; Ethanol oxidation; Sol–gel; Modified carbon electrodes

1. Introduction

Fuel cells are very promising devices for the production of electrical energy due to the high efficiency of the electrochemical combustion in comparison with the chemical one, minimizing the formation of unwanted by-products that contaminate the atmosphere. In addition, the use of hydrogen as the fuel has allowed the development of several systems that are very convenient for a variety of applications. However, the production and handling of this material is a complex and expensive task and alternative fuels have been investigated in recent years, particularly methanol and ethanol, the latter being the best choice from the environmental viewpoint.

In the meantime, the anode material of this kind of device constitutes a major technological problem. Platinum shows the highest activity for the electro-oxidation of ethanol; but the

performance of pure Pt electrodes is not sufficient due to the formation of strongly adsorbed intermediates which block the anode surface. At the moment, efforts are centered in the reduction of the amount of adsorbed intermediates by the addition of co-catalysts. Watanabe and Motoo [1] described a bi-functional mechanism for methanol oxidation which is related to the formation of OH^\bullet by ruthenium atoms at low potentials which transform the CO adsorbed on platinum into CO_2 . Other authors [2,3] have also proposed that Ru enhances methanol oxidation through an electronic effect on neighboring Pt atoms (the ligand effect). In those mechanisms, it has been proposed that Ru may accelerate the adsorption and dehydrogenation of methanol on Pt sites at low potentials or it may weaken the Pt–CO bond allowing the oxidation of CO at lower potentials.

Following these mechanisms, several techniques of deposition have been proposed to fix Pt and Ru on different substrates. One that is largely used was proposed by Bönemann [4] and recent reports have demonstrated that the sol–gel [5–7] method is an efficient and simple technique to produce carbon powder composites containing Pt and Ru with the desired composition for both methanol and ethanol oxidation in acidic medium and

* Corresponding author. Tel.: +55 11 4437 1600x434;

fax: +55 11 4437 1600x804.

E-mail address: hugo.suffredini@ufabc.edu.br (H.B. Suffredini).

for the deposition of nanoparticles with different but controlled compositions on powder substrates for fuel cell applications [8,9].

PtRu-based materials have shown promising results for the electrochemical oxidation of alcohols in acidic media [10–12]. Some authors studied the effect of the catalyst composition on the ethanol oxidation reaction [13,14] as well as the influence of the deposition method on the catalytic activity of these composites toward methanol oxidation [15,16]. Nevertheless, the use of some other metal or metallic oxide is still needed for further improvement of the catalytic activity of these anodes.

In this sense, using the molecular orbital theory, Shiller and Anderson [17] studied the effects of chemisorbed and substitutional Ge, Sn and Pb on CO adsorption on Pt(111). The substitutional bonding of M, M–OH and M–O, where M = Ge, Sn and Pb, in the Pt(111) surface is predicted to cause small weakening or slight strengthening of the CO adsorption energies. Adsorbed Ge, Sn and Pb atoms, on the other hand, have a marked effect, weakening the CO adsorption energy at neighboring sites by ~ 0.09 – 0.13 eV. Later, Biswas et al. [18] observed that a graphite-based Pt electrode modified with In + Pb mixed oxide exhibited a considerable level of electrocatalytic activity toward methanol electro-oxidation in a H_2SO_4 0.5 mol L^{-1} + CH_3OH 1 mol L^{-1} mixed solution. Also, El-Shafei et al. [19] showed that the addition of Pb and Tl ad-atoms to a Pt sheet increases the oxidation rate of ethanol in alkaline medium by a factor of about 15 compared with pure Pt.

Recently, Golikand et al. [20] studied the oxidation of methanol in acidic media at a lead electrode modified by Pt, Pt–Ru or Pt–Sn microparticles dispersed into an electropolymerized poly(*o*-phenylenediamine) (PoPD) film. The reactivity of the electrodes was greatly enhanced when an optimized mixture of Pt–Sn and Pt–Ru microparticles were electrochemically deposited inside the PoPD film. However, the influence of the Pb substrate on the catalytic activity of the electrodes was not investigated.

Furthermore, Casado-Rivera et al. [21] studied the electrocatalytic activity of a wide range of ordered intermetallic phases for a variety of potential fuels (i.e. methanol, ethanol, ethylene glycol and acetic acid). The PtBi, PtIn and PtPb ordered intermetallic phases appeared to be the most promising electrocatalysts tested for fuel cell applications. In particular, PtPb showed an onset potential that was 240 mV less positive and a peak current density ~ 20 times higher than those observed for Pt in the case of ethanol oxidation. More recently, intermetallic PtPb unsupported nanoparticles (~ 16 nm) were synthesized by the chemical reduction of dimethyl(1,5-cyclooctadiene)platinum and lead(II) 2-ethylhexanoate by sodium naphthalide in tetrahydrofuran or diglyme [22]. The PtPb nanoparticles exhibited a remarkable ability to oxidize formic acid, with a high mass activity and onset potentials similar to those reported previously for bulk PtPb electrodes [21].

Also, Li and Pickup [23] have recently reported the preparation of a composite by the incorporation of Pb to commercial Pt or Pt/Ru powder catalysts. The initial addition of $\text{Pb}(\text{NO}_3)_2$ dissolved in water to the commercial catalysts dispersed in water and under stirring was followed by an excess of a NaBH_4 aque-

ous solution. The product was collected by filtration, washed and then dried at room temperature in a vacuum oven. These catalysts exhibited significantly enhanced catalytic activity for ethanol oxidation relative to their parent Pt and Pt/Ru powders. The authors suggested that the primary mode of action of the Pb ad-atoms in promoting ethanol oxidation is presumably the removal of adsorbed CO by the bi-functional mechanism that operates for many different Pt alloys.

On the other hand, several works have reported the advantages of using boron-doped diamond (BDD) electrodes in electrochemistry. The BDD electrodes possess electrochemical properties significantly different from other allotropic forms of carbon that are used as electrode materials, such as pyrolytic carbon, graphite and/or vitreous carbon. Thus, BDD shows a very large electrochemical potential window in either aqueous or non-aqueous media [24,25], enhanced chemical and mechanical stability and high corrosion resistance [26]. Salazar-Banda and co-workers [28,29] and González-González et al. [30] used the BDD electrode as substrate to produce composite anodes for alcohol oxidation demonstrating the good performance of these materials. Moreover, the sol–gel method has proved to be a simple, efficient and very appropriate technique to produce nanometric catalytic deposits with the desired composition on BDD film electrodes [27–29], on BDD powder [31] and on carbon powder surfaces [5,6,32] at a low cost.

Thus, the aim of this work is to report for the first time the deposition of lead oxide-based catalyst by the sol–gel method on carbon powder and fixed on a BDD substrate to produce anodes containing Pt, Ru, Ir, Pb and carbon with 10% of total catalyst load. The characterization of the powders was performed by X-ray diffraction (XRD) and energy dispersive X-ray (EDX) analysis and the study of the electrochemical ethanol oxidation reaction was carried out by cyclic voltammetry, quasi-stationary polarization experiments (Tafel plots) and chronoamperometry for the prepared composite materials fixed on a BDD substrate.

2. Experimental

2.1. Reagents and apparatus

The electrochemical experiments were performed in a one-compartment Pyrex[®] glass cell provided with three electrodes. The reference system was a hydrogen electrode in the same solution (HESS) and the auxiliary one was a 2 cm^2 Pt foil. The BDD electrodes used as substrate were produced by the Center Suisse d'Electronique et de Microtechnique SA (CSEM), Neuchâtel, Switzerland, on Si wafers using the hot filament chemical vapor deposition technique. The final boron content of the electrodes was of the order of 4500–5000 ppm. The supporting electrolyte was a H_2SO_4 0.5 mol L^{-1} solution (Merck[®]) also containing ethanol 1.0 mol L^{-1} (Synth[®]). All electrochemical measurements were carried out using an EG&G Princeton Applied Research (PAR) Potentiostat/Galvanostat model 273A coupled to an IBM-PC compatible microcomputer and the EG&G PAR model 270 Research Electrochemistry Software.

The preparation of the sol–gel solutions is described below. The platinum solution (as an example) was prepared adding

0.0099 g of the Pt(II) acetylacetonate (Aldrich®) to 25 cm³ of a liquid mixture constituted by ethanol (Synth® 98°) and acetic acid (Merck® P.A.) 3:2 (v/v) while the ruthenium, iridium and lead solutions were prepared using the same procedure but adding the necessary acetylacetonates quantities (Aldrich®). The sol–gel solutions were subjected to ultrasonic treatment (Thorniton® Sonicator) for 5 min (homogenization step). The final concentration of each one of these organometallic solutions was $1.0 \times 10^{-3} \text{ mol L}^{-1}$. The carbon black powder used was a Vulcan® XC72R while a 5% commercial Nafion® solution (DuPont) was purchased from Aldrich®.

2.2. Composite preparation

The composites containing Pt, Ru, Ir, Pb and C were prepared using a fixed mass proportion of metals Pt:Ru (50:50), Pt:Ir (50:50), Pt:Pb (50:50), Pt:Ru:Ir (50:25:25), Pt:Ru:Pb (50:25:25) and Pt:Pb:Ir (50:25:25) and carbon powder as support. The catalyst mass load was fixed in 10%, with respect to the carbon powder.

The depositions were carried out according to a procedure reported elsewhere [5], by putting the dry carbon powder (0.13 g) into a beaker and covering this powder with small amounts of the mixed organometallic solutions (1–2 cm³ by step), producing a

“black mud” without excess of liquid. After the quasi-total evaporation of the liquid from the “black mud” (at room temperature) further amounts of 1 cm³ were added. This procedure (polymerization step) was repeated until a load of 10% of catalysts was attained. The carbon powder impregnated with the organometallic compounds was then subjected to a thermal treatment at 400 °C for 1 h under argon atmosphere.

2.3. The use of diamond as substrate

The synthesized composites were fixed onto a BDD electrode following the procedure described by Schmidt et al. [33]. Firstly, a 5 wt% Nafion solution was diluted ten times in deionised water. Then, 0.008 g of the composite was added to 1 cm³ of water and 0.20 cm³ of the diluted Nafion® solution. The resulting system was placed in an ultrasonic bath for 3 min to disperse the powder in the solution. Finally, 0.02 cm³ of the obtained dispersion were transferred onto a diamond electrode with geometric area of 0.125 cm². The deposited suspension was then dried for 60 min at 80 °C to complete evaporation of the solvents, thereby obtaining a thin layer of the powder catalyst sticking to the diamond electrode surface. Also, a Pt/C commercial powder (E-TEK) with 10% catalyst mass loading was used for comparison with the composites prepared in this work.

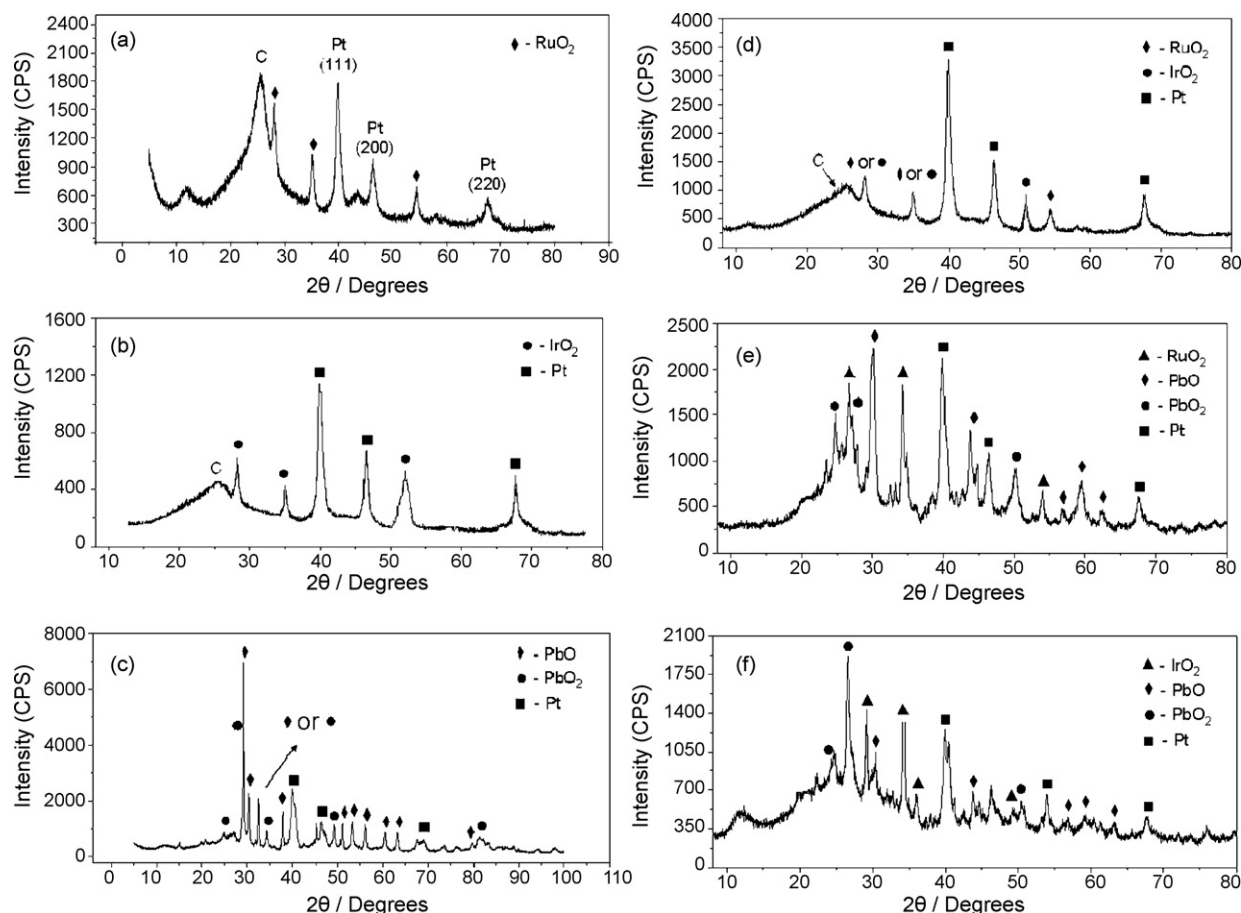


Fig. 1. X-ray diffraction spectra taken at 2° min^{-1} of scan rate for: (a) Pt-RuO₂/C, (b) Pt-IrO₂/C, (c) Pt-PbO_x/C, (d) Pt-(RuO₂-IrO₂)/C, (e) Pt-(RuO₂-PbO_x)/C and (f) Pt-(IrO₂-PbO_x)/C. The graph (a) also shows the different Pt polycrystalline faces (1 1 1), (2 0 0) and (2 2 0), that are the same to all composites.

3. Results and discussion

3.1. Physical characterization

Fig. 1 shows the XRD patterns obtained for all composites prepared in this work together with the corresponding indication of the main peaks and their identification by comparison with the Joint Committee of Power Diffraction Standards (JCPDS) cards. It can be observed from that figure that in all cases Pt was deposited as a metal in the polycrystalline form (JCPDS #04-0802) showing the peaks corresponding to the main three crystallographic planes (1 1 1), (2 0 0) and (2 2 0). This is in agreement with previous reports on the sol–gel deposition of Pt on carbon powder [29,31,32] and on Pt–Ru alloys synthesized in two ways: on the one hand, polycrystalline Pt–Ru reference samples prepared by arc melting starting from appropriate mixtures of Pt and Ru powders and on the other hand, nanocrystalline Pt–Ru particles of about 8 nm electrochemically deposited in carbon/Nafion™ layers on glassy carbon discs [34].

On the other hand, the composites containing Ru and Ir show several peaks corresponding to RuO₂ (JCPDS #43-1027) and IrO₂ (JCPDS #43-1019), respectively, which are the expected structures when the deposition process is the sol–gel method [35]. In addition, Pb was deposited as a mixture of PbO (JCPDS #38-1477) and PbO₂ (JCPDS #37-1517). Thus, the nomenclature of all Pb-containing compounds is designed by “PbO_x”.

EDX measurements were also used to calculate the atomic proportions of the elements present in the composites. The procedure adopted here for those calculations consisted in selecting three points in different regions of the sample to minimize the composition deviations and to determine the composition in each one to obtain a mean value. EDX analyses is presented in Fig. 2 and revealed that Pb is preferentially deposited as compared to Pt, as indicated by the compositions collected in Table 1. While for the other composites that were studied, a very good agreement between the experimental and the expected theoretical values is observed, showing a negligible surface segregation during preparation, as already reported for sol–gel prepared catalysts containing Pt, Ru and/or Ir in their composition [29,31,32].

The values of the crystallite dimensions obtained by using the software WinFit version 1.2 [36] and the Scherrer relationship on the XRD spectra are included in Table 1. These values confirm the nanometric character of the composites. In fact, the characteristic dimension of metal clusters employed in fuel cells is in the size range of a few nanometers. In this sense, it was observed that small Pt particles (from 3.5 to 4.0 nm) have higher

intrinsic activity for methanol oxidation due to their high activity for methanol dehydrogenation step [37]. However, a lower tolerance to CO poisoning was confirmed by FTIR spectroscopy for very small particles (ca. 1.7 nm), evidencing that the CO₂ production is shifted toward positive potentials compared to large particles [38]. Also, the model for *perfect* cubooctahedral particles suggested restricted CO mobility (reduced activity) at Pt nanoparticles below ca. 2 nm size and a transition toward fast diffusion (enhanced activity) when the particle size exceeds 3 nm [39]. Consequently, as the size of the prepared catalysts is in the range between 3.3 and 6.9 nm, this small size (but not smaller than 2 nm) could probably be responsible for the enhanced catalytic activity toward ethanol oxidation presented by these materials.

3.2. Electrochemical studies

Fig. 3 shows the cyclic voltammetric studies carried out in H₂SO₄ 0.5 mol L⁻¹ solution (dotted lines) and in the same acidic solution but, in the presence of CH₃CH₂OH 1.0 mol L⁻¹ (full lines). The blank responses show the presence of Pt due to the inhibited signals of the adsorption–desorption of hydrogen on the exposed Pt in each catalyst.

Meanwhile, in the presence of ethanol, higher current densities are observed on the Pt–PbO_x/C, Pt–(RuO₂–IrO₂)/C and Pt–(RuO₂–PbO_x)/C composites (i.e. ~80 A (g Pt)⁻¹ taken at 400 mV). On the contrary, the Pt–(IrO₂–PbO_x) catalyst showed the lowest current density (i.e. ~10 A (g Pt)⁻¹ taken at 400 mV), while a middle catalytic performance is observed on the Pt–RuO₂ and Pt–IrO₂ binary catalysts with current density values of ~50 A (g Pt)⁻¹ (taken at 400 mV). It can also be observed in Fig. 3 that the ethanol oxidation has onset potentials (taken at *i* = 0.1 mA cm⁻¹) in the range of 150–200 mV versus HESS in almost all the prepared catalysts except on the Pt–(IrO₂–PbO_x)/C composite, which presents an onset potential of about 500 mV versus HESS. So, in view of these results, it is important to notice that the preparation of composites containing simultaneously platinum, lead and iridium compounds leads to a very bad catalyst and this mixture must be avoided. However, this effect could be due to the lack of oxygenated species at the electrode surface provided by the Ru at low potentials, but it is not clear and further studies are required for better understanding.

Otherwise, the good catalytic performance for the ethanol oxidation presented by binary and other ternary catalytic compositions observed in the cyclic voltammetric experiments encouraged the study in quasi-stationary conditions.

Table 1
Expected and EDX measured compositions and crystallite dimensions for the different composites

Composite	Expected composition	Measured composition ^a	Crystallite dimension (nm)
Pt–RuO ₂ /C	50% Pt–50% Ru	49% Pt–51% Ru	4.8
Pt–IrO ₂ /C	50% Pt–50% Ir	56% Pt–44% Ir	5.7
Pt–PbO _x /C	50% Pt–50% Pb	40% Pt–60% Pb	3.4
Pt–(RuO ₂ –IrO ₂)/C	50% Pt–25% Ru–25% Ir	52% Pt–22% Ru–26% Ir	6.9
Pt–(RuO ₂ –PbO _x)/C	50% Pt–25% Pb–25% Ru	38% Pt–40% Pb–22% Ru	6.8
Pt–(IrO ₂ –PbO _x)/C	50% Pt–25% Pb–25% Ir	33% Pt–40% Pb–27% Ir	3.3

^a Mean EDX value at three different points of the sample.

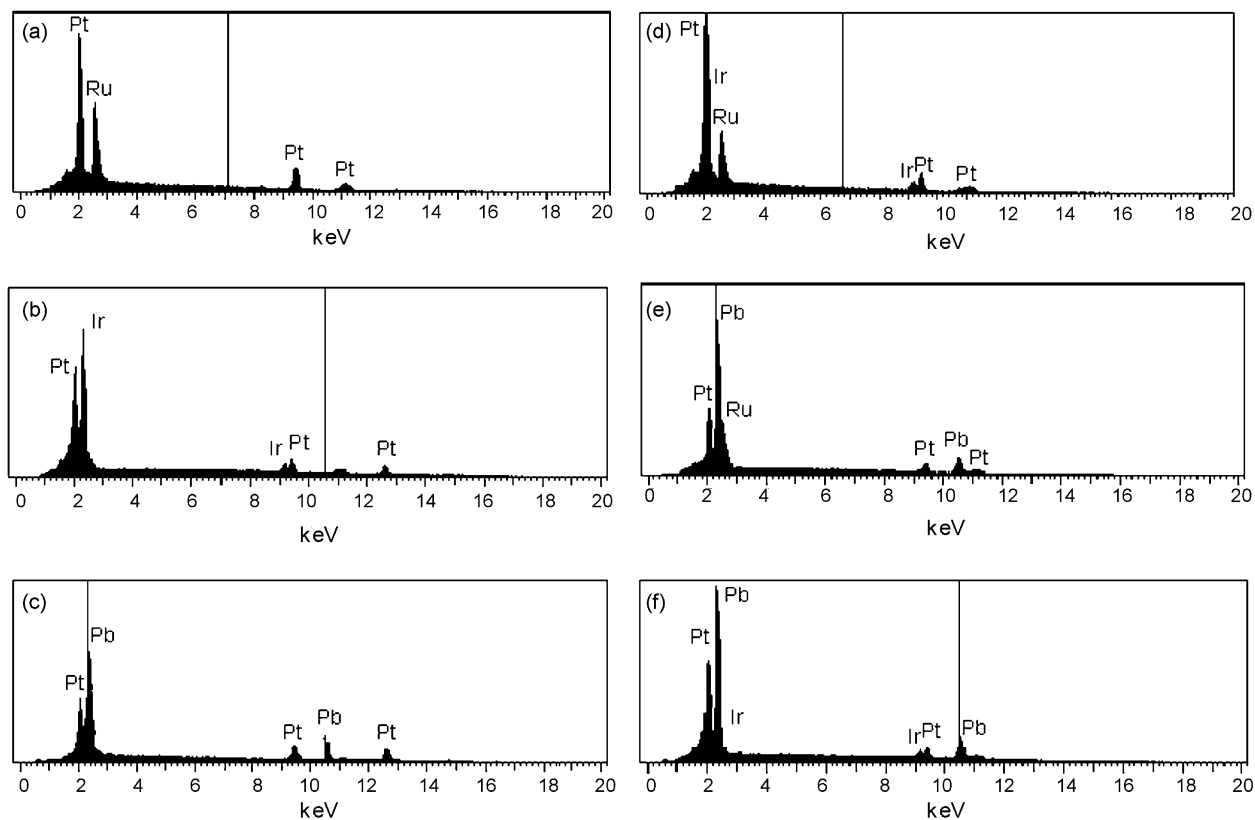


Fig. 2. EDX spectra for: (a) Pt-RuO₂/C, (b) Pt-IrO₂/C, (c) Pt-PbO_x/C, (d) Pt-(RuO₂-IrO₂)/C, (e) Pt-(RuO₂-PbO_x)/C and (f) Pt-(IrO₂-PbO_x)/C. The carbon response was omitted due to the very intense signal if compared to the metallic compounds.

So, aiming to compare the catalytic effect of the composites in the kinetic controlled process, Fig. 4 shows the quasi-steady-state polarization curves presented as Tafel plots that were carried out in potentiostatic mode, at 20 °C in H₂SO₄ 0.5 mol L⁻¹ + CH₃CH₂OH 1.0 mol L⁻¹ aqueous solution using the potentiostatic current values measured after 300 s of polarization at each selected potential value (each 20 mV) in the range from 50 to 900 mV. This kind of measurement is a very useful tool for the study of the electrochemical oxidation of ethanol and was successfully used for this purpose in recent papers [6,29,31]. It can be observed that the Pt/C commercial composite showed a response with the “quasi-instantaneous” intermediates formation during the oxidation, causing low oxidation activity with an onset potential of 622 mV. Again, the Pt-(IrO₂-PbO_x) catalyst showed a low catalytic activity if compared with the other materials prepared in this study with an onset potential of the oxidation reaction of 439 mV, yet, this activity is somewhat better than the one presented by catalyst containing only Pt in their composition with an onset potential more negative in ~180 mV. So, apparently, the combination of IrO₂ with PbO_x disfavors the catalytic activity for the ethanol oxidation showing a non-synergic behavior.

On the other hand, the composites Pt-(RuO₂-PbO_x)/C and Pt-(RuO₂-IrO₂)/C started the oxidation process in very low potentials (155 and 178 mV, respectively), presenting good performance to promote the ethanol oxidation. Comparing the performance of the catalysts, the composite Pt-(RuO₂-PbO_x)/C presented a gain of about 467 mV in the onset potential as

compared to the Pt/C composite and as a consequence, very high currents can be obtained on this catalyst at low potentials. This elevated gain in the onset potential (467 mV) is higher than the recently reported on the Pt/Pb catalysts prepared by deposition of Pb on commercial Pt [23] and on Pt-CeO₂/C, composites prepared by a solid-state reaction under microwave irradiation [40,41], which were lower than that obtained on the Pt catalyst in approximately 100 mV. These onset potentials (155 and 178 mV) are also more negative than those recently reported on ternary Pt-Sn-Ru/C (1:1:0.3 and 1:1:1) catalysts synthesized by reduction of precursors with formic acid (i.e. in the range of 250–280 mV versus RHE) [42].

Likewise, the binary composites showed a middle catalytic activity for the studied reaction with onset potentials in the range of 200–240 mV. Consequently, as the catalyst containing lead oxide showed the best performance between the binary catalysts, the utilization of this oxides mixture (PbO_x) points out the importance of their utilization in studies about alcohols oxidation. The lower onset potentials and enhanced catalytic activities of the binary and ternary catalysts containing Pb as compared to Pt could be in part due to the oxidation of adsorbed intermediates by water that must be activated by Pb oxides, but, in view of the non-synergic behavior presented by the catalyst Pt-(IrO₂-PbO_x) (absence of Ru, known as water activator at low potentials), it is more probably due to a weakening of the CO adsorption bond at neighboring sites of Pt as already calculated for Pb bonding in the Pt(1 1 1) surface [17].

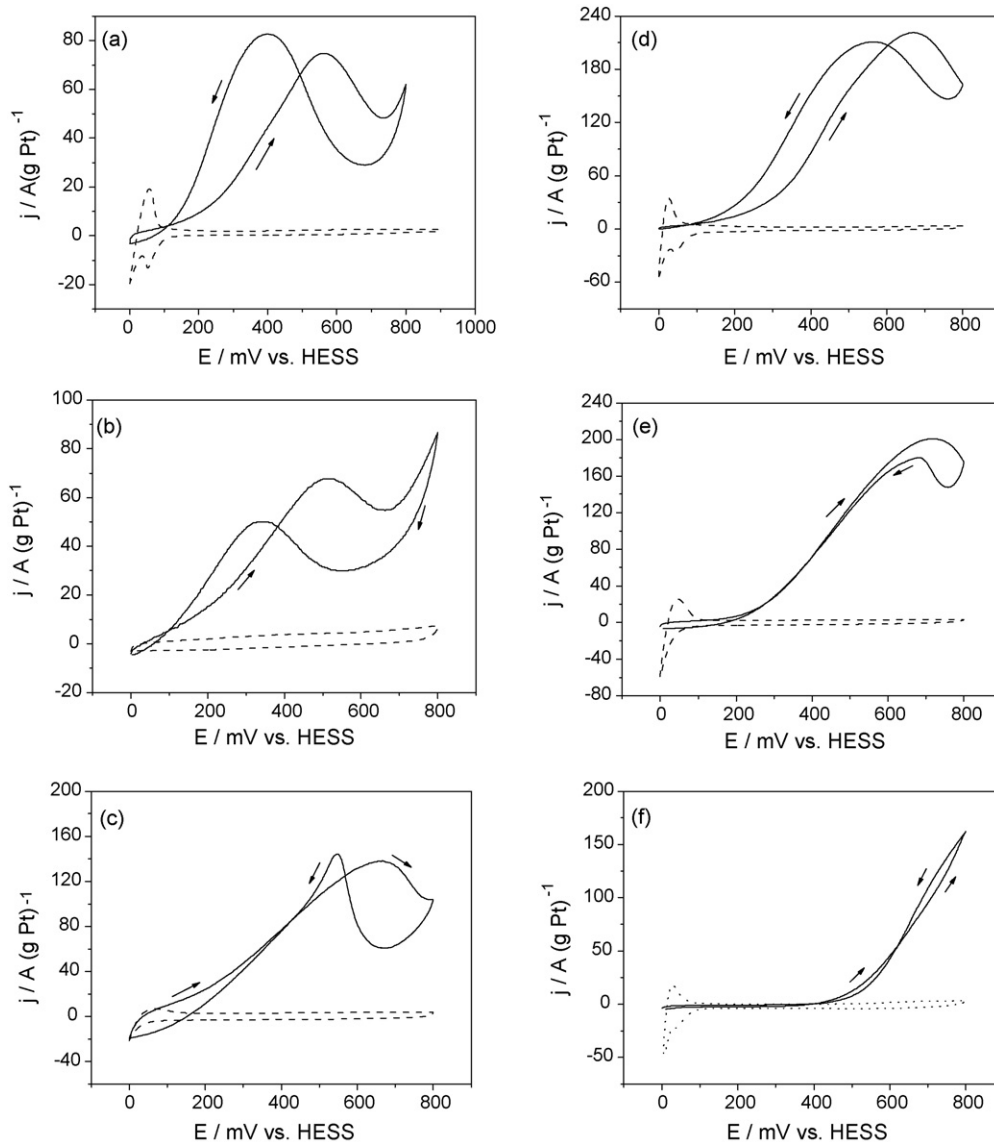
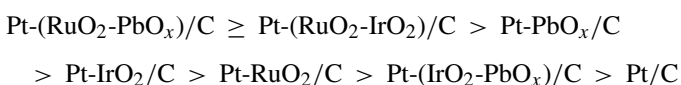


Fig. 3. Cyclic voltammetric responses of the composites: (a) Pt-RuO₂/C, (b) Pt-IrO₂/C, (c) Pt-PbO_x/C, (d) Pt-(RuO₂-IrO₂)/C, (e) Pt-(RuO₂-PbO_x)/C and (f) Pt-(IrO₂-PbO_x)/C in H₂SO₄ 0.5 mol L⁻¹ (dotted lines) and in a mixture of H₂SO₄ 0.5 mol L⁻¹ + CH₃CH₂OH 1.0 mol L⁻¹ (solid lines).

It is worth to mention that a minimum value of current was fixed to properly determine and compare the onset potential values for the ethanol oxidation reaction at the different catalysts. Thus, all onset potential values discussed and obtained from Fig. 4 were taken at $I = 2E^{-5}$ A.

The catalysts Pt-(RuO₂-PbO_x), Pt-(RuO₂-IrO₂), Pt-PbO_x/C, Pt-RuO₂/C and Pt-IrO₂ exhibited significantly enhanced catalytic activity for the ethanol oxidation relative to the observed on a Pt commercial catalyst. As a matter of fact, the addition of the metallic oxides by the sol-gel route to Pt showed to be a very interesting way to prepare materials with high catalytic activity for direct ethanol fuel cell systems.

The succession of the catalytic activity for the ethanol oxidation of all materials studied was:



The materials prepared were also submitted to an ethanol oxidation process in a fixed potential of 550 mV versus HESS for 2600 s. The results are presented in Fig. 5 and show that the composites Pt-(RuO₂-IrO₂)/C and Pt-(RuO₂-PbO_x)/C, represented in this graph by “1” and “2”, respectively, exhibit higher current densities for the same applied potential for the studied time. Notwithstanding, a slower and continuous current decay is observed in the Pt-(RuO₂-PbO_x) catalyst due to a smaller poisoning of the material as the process advances. On the contrary, the curve related to the Pt/C composite tends to zero. Moreover, the synergic effect of the addition of lead oxides to Pt is observed again in Fig. 5 (curve 3), which presents pseudo-current density higher than the presented by the other two binary catalysts (i.e. Pt-IrO₂ and Pt-RuO₂). In view of the excellent catalytic activities observed on the lead oxide-based composites, further studies will be carry out to understand the oxidation mechanism and other fuels must be tested to determine their catalytic activity.

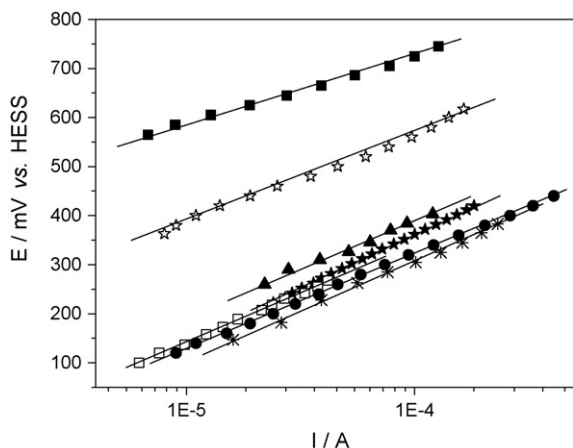


Fig. 4. Tafel Plots recorded in potentiostatic mode in H_2SO_4 0.5 mol L^{-1} + $\text{CH}_3\text{CH}_2\text{OH}$ 1.0 mol L^{-1} for: Pt/C E-Tek (■), Pt-(IrO_2 - PbO_x)/C (☆), Pt- RuO_2 /C (▲), Pt- IrO_2 /C (★), Pt- PbO_x /C (□), Pt-(RuO_2 - IrO_2)/C (●) and Pt-(RuO_2 - PbO_x)/C (⋈). $T = 20^\circ\text{C}$.

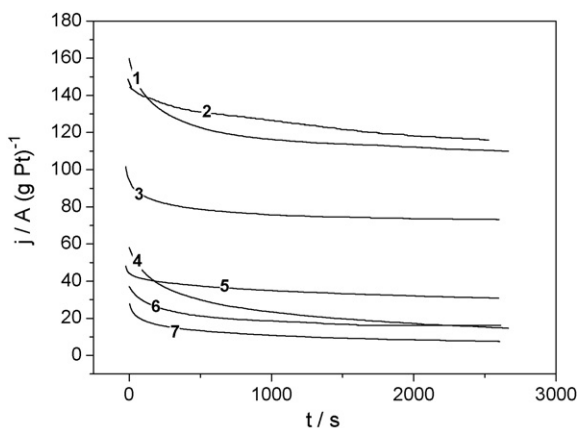


Fig. 5. Current–time responses measured at 550 mV vs. HESS for: (1) Pt-(RuO_2 - IrO_2)/C, (2) Pt-(RuO_2 - PbO_x)/C, (3) Pt- PbO_x /C, (4) Pt- RuO_2 /C, (5) Pt- IrO_2 /C, (6) Pt-(IrO_2 - PbO_2)/C and (7) Pt/C E-Tek in a H_2SO_4 0.5 mol L^{-1} + $\text{CH}_3\text{CH}_2\text{OH}$ 1.0 mol L^{-1} aqueous solution.

4. Conclusions

The physical characterization of the composites demonstrates that the preferential deposits are the polycrystalline Pt, IrO_2 , RuO_2 and a mixture of PbO and PbO_2 . The crystallite dimensions are about 5 nm, showing the nanometric character of the composites. The relative compositions were different from the theoretical values when the composite have Pb in the composition, due to the preferential deposition of Pb if compared to Pt.

The electrochemical oxidation of ethanol in acidic media investigated by cyclic voltammetry showed higher current densities on the Pt- PbO_x /C, Pt-(RuO_2 - IrO_2)/C and Pt-(RuO_2 - PbO_x)/C composites while the Pt-(IrO_2 - PbO_x) catalyst showed the lowest current density. Moreover, quasi-steady-state polarization curves showed that the composites Pt-(RuO_2 - PbO_x)/C and Pt-(RuO_2 - IrO_2)/C started the oxidation process in very low potentials (155 and 178 mV, respectively), presenting good performance to promote the ethanol oxidation. On the contrary, the

combination of IrO_2 with PbO_x disfavors the catalytic activity for the ethanol oxidation, showing a non-synergic behavior. Thus, the order of reactivity was determined as being:

$$\begin{aligned} & \text{“Pt-(RuO}_2\text{-PbO}_x\text{)}/\text{C} \approx \text{Pt-(RuO}_2\text{-IrO}_2\text{)}/\text{C} > \text{Pt-PbO}_x\text{/C} \\ & > \text{Pt-IrO}_2\text{/C} > \text{Pt-RuO}_2\text{/C} > \text{Pt-(IrO}_2\text{-PbO}_x\text{)}/\text{C} > \text{Pt/C”} \end{aligned}$$

Consequently, the catalysts Pt-(RuO_2 - PbO_x), Pt-(RuO_2 - IrO_2), Pt- PbO_x /C, Pt- RuO_2 /C and Pt- IrO_2 exhibited significantly enhanced catalytic activity for the ethanol oxidation (observed as higher current activities and less positive reaction onset potentials) when compared to the observed on a Pt commercial catalyst. In this work, the oxidation products were not analyzed and the results have considered only the catalytic activities. As a matter of fact, the addition of metallic oxides by the sol-gel route to Pt showed to be a very interesting way to prepare materials with high catalytic activity for direct ethanol fuel cell systems. Thus, the good results observed on the lead oxide-based catalysts are in good agreement with the continuity of the research.

Acknowledgements

Prof. Nicolaos Vatisstas (University of Pisa) for useful discussions, FAPESP (procs. 01/14320-0 and 06/50692-2) and CNPq for the financial support.

References

- [1] M. Watanabe, S. Motoo, *J. Electroanal. Chem.* 60 (1975) 267–273.
- [2] M. Krausa, W. Vielstich, *J. Electroanal. Chem.* 379 (1994) 307–314.
- [3] Y.Y. Tong, H.S. Kim, P.K. Babu, P. Waszczuk, A. Wieckowski, E. Oldfield, *J. Am. Chem. Soc.* 124 (2002) 468–473.
- [4] H. Bönemann, W. Brijoux, R. Brinkmann, E. Dinjus, R. Fretzen, T. Jouben, B. Korall, *J. Mol. Catal.* 74 (1992) 323–333.
- [5] H.B. Suffredini, V. Tricoli, L.A. Avaca, N. Vatisstas, *Electrochem. Commun.* 6 (2004) 1025–1028.
- [6] H.B. Suffredini, V. Tricoli, N. Vatisstas, L.A. Avaca, *J. Power Sources* 158 (2006) 124–128.
- [7] C. Arbizzani, S. Beninati, E. Manferrari, F. Soavi, M. Mastragostino, *J. Power Sources* 161 (2006) 826–830.
- [8] N.R. Elezović, B.M. Babić, N.V. Krstajić, L.M. Gajić-Krstajić, Lj.M. Vračar, *Int. J. Hydrogen Energy* 32 (2007) 1991–1998.
- [9] H. Song, X. Qiu, F. Li, W. Zhu, L. Chen, *Electrochem. Commun.* 9 (2007) 1416–1421.
- [10] E. Frackowiak, G. Lota, T. Cacciaguerra, F. Béguin, *Electrochem. Commun.* 8 (2006) 129–132.
- [11] P. Sivakumar, R. Ishak, V. Tricoli, *Electrochim. Acta* 50 (2005) 3312–3319.
- [12] S. Rojas, F.J. García-García, S. Järas, M.V. Martínez-Huerta, J.L.G. Fierro, M. Boutonnet, *Appl. Catal. A: Gen.* 285 (2005) 24–35.
- [13] G.A. Camara, R.B. de Lima, T. Iwasita, *J. Electroanal. Chem.* 585 (2005) 128–131.
- [14] G.A. Camara, R.B. de Lima, T. Iwasita, *Electrochem. Commun.* 6 (2004) 812–815.
- [15] M.H. Pournaghi-Azar, B. Habibi-A, *J. Electroanal. Chem.* 580 (2005) 23–34.
- [16] S.T. Kuk, A. Wieckowski, *J. Power Sources* 141 (2005) 1–7.
- [17] P. Shiller, A.B. Anderson, *Surf. Sci.* 236 (1990) 225–232.
- [18] P.C. Biswas, T. Ohmori, M. Enyo, *J. Electroanal. Chem.* 305 (1991) 205–215.
- [19] A.A. El-Shafei, S.A. Abd El-Maksoud, M.N.H. Moussa, *J. Electroanal. Chem.* 336 (1992) 73–83.

- [20] A.N. Golikand, S.M. Golabi, M.G. Maragheh, L. Irannejad, J. Power Sources 145 (2005) 116–123.
- [21] E. Casado-Rivera, D.J. Volpe, L.R. Alden, C. Lind, C. Downie, T. Vázquez-Alvarez, A.C.D. Angelo, F.J. DiSalvo, H.D. Abruña, J. Am. Chem. Soc. 126 (2004) 4043–4049.
- [22] L.R. Alden, D.K. Han, F. Matsumoto, H.D. Abruña, F.J. DiSalvo, Chem. Mater. 18 (2006) 5591–5596.
- [23] G. Li, P.G. Pickup, Electrochim. Acta 52 (2006) 1033–1037.
- [24] H.B. Suffredini, S.A.S. Machado, L.A. Avaca, J. Braz. Chem. Soc. 15 (2004) 16–21.
- [25] L.F. Li, D.A. Totir, B. Miller, G. Chottiner, A. Argoitia, J.C. Angus, D.A. Scherson, J. Am. Chem. Soc. 119 (1997) 7875–7876.
- [26] G.M. Swain, J. Electrochem. Soc. 141 (1994) 3382–3393.
- [27] G.R. Salazar-Banda, H.B. Suffredini, L.A. Avaca, J. Braz. Chem. Soc. 16 (2005) 903–906.
- [28] H.B. Suffredini, G.R. Salazar-Banda, S.T. Tanimoto, M.L. Calegario, S.A.S. Machado, L.A. Avaca, J. Braz. Chem. Soc. 16 (2006) 257–264.
- [29] G.R. Salazar-Banda, H.B. Suffredini, M.L. Calegario, S.T. Tanimoto, L.A. Avaca, J. Power Sources 162 (2006) 9–20.
- [30] I. González-González, D.A. Tryk, C.R. Cabrera, Diam. Relat. Mater. 15 (2006) 275–278.
- [31] G.R. Salazar-Banda, K.I.B. Eguiluz, L.A. Avaca, Electrochem. Commun. 9 (2007) 59–64.
- [32] M.L. Calegario, H.B. Suffredini, S.A.S. Machado, L.A. Avaca, J. Power Sources 156 (2006) 300–305.
- [33] T.J. Schmidt, H.A. Gasteiger, G.D. Stab, P.M. Urban, D.M. Kolb, R.J. Behm, J. Electrochem. Soc. 145 (1998) 2354–2358.
- [34] M.S. Löffler, H. Natter, R. Hempelmann, K. Wippermann, Electrochim. Acta 48 (2003) 3047–3051.
- [35] F.I. Mattos-Costa, P. de Lima-Neto, S.A.S. Machado, L.A. Avaca, Electrochim. Acta 44 (1998) 1515–1523.
- [36] S. Krumm, Comp. Geosci. 25 (1999) 489–499.
- [37] Z. Liu, M. Shamsuzzoha, E.T. Ada, W. Matthew Reichert, D.E. Nikles, J. Power Sources 164 (2007) 472–480.
- [38] F. Maillard, E. Savinova, P.A. Simonov, V.I. Zaikovskii, U. Stimming, J. Phys. Chem. B 108 (2004) 17893–17904.
- [39] F. Maillard, M. Eikerling, O.V. Cherstiouk, S. Schreier, E. Savinova, U. Stimming, Faraday Discuss. 125 (2004) 357–377.
- [40] C. Xu, P.K. Shen, J. Power Sources 142 (2005) 27–29.
- [41] C. Xu, R. Zeng, P.K. Shen, Z. Wei, Electrochim. Acta 51 (2005) 1031–1035.
- [42] E. Antolini, F. Colmati, E.R. Gonzalez, Electrochem. Commun. 9 (2007) 398–404.